Self-consistent model of a nanoscale semiconductor laser using Green and Wigner functions in two bases

Philip Weetman and Marek S. Wartak
Department of Physics and Computer Science, Wilfrid Laurier University, Waterloo, Ontario N2L 3C5, Canada
(Received 1 March 2007; published 26 July 2007)

We report on the development of a self-consistent nanoscale semiconductor laser model. Wigner functions are used for modeling the carrier dynamics and the effect of the boundary conditions. The Green functions are used for interband polarizations, which we use to derive the optical susceptibility. We begin with a generalized approach applicable to different nanosystems with a flexible band-structure-type information and finish with an example of a quantum well laser using a combination of parabolic and Lüttinger-Köhn band structure approximations. The novelty of this model is its ability to self-consistently incorporate spectral and dynamical characteristics for a semiconductor laser. In particular, an example will be presented where a nonequilibrium correction term for the standard susceptibility equation is derived.

DOI: 10.1103/PhysRevB.76.035332 PACS number(s): 73.21.Fg, 73.43.Cd, 73.63.Hs, 78.67.De

I. INTRODUCTION

For a realistic nanophotonic laser model, it is necessary to describe both the spectral (susceptibility) and dynamic (carrier transport) properties of the system simultaneously. Examples of such models are drift diffusion or rate equations combined with equilibrium gain formulations.[1–4] These require a large amount of assumptions and parameters which reduces their predictive power. Another possible approach would be a fully microscopic model using Green functions. In that sort of model, we would need to define Green functions in the contact regions to couple to the rest of the system as the way to incorporate boundary conditions.[5,6]

In this paper, we will present a combined Wigner and Green function model of nanophotonic systems. The rationale for the approach is that the Wigner functions are a very convenient form to describe the carrier dynamics and boundary conditions,[1,7–11] whereas the Green functions (or the simplified density matricies) are well suited for the polarizations and susceptibility.[12–15] The starting point for both functions is the one-particle nonequilibrium Green functions in general position space with their evolution described by Dyson's equations.

In the first representation, we express the general Green functions in position space in the *eigenfunction basis* (the eigenfunctions of the noninteracting Hamiltonian of the system). Dyson's equations are also transformed into the eigenfunction basis. In the second representation, we express the general Green functions in position space in the *band basis*. This is defined by integrating out all spatial variations that quickly vary with respect to the lattice size. The Green functions in this basis are then transformed into the *Wigner functions* by applying the Wigner-Weyl transformation. Either representation can be used to completely model the system. For example, in our previous work,[1,11,16] we carried out all our analyses solely with Wigner functions in the band basis representation.

The structure of the paper is as follows. In Sec. II we describe the Green functions in the eigenfunction basis and the Wigner functions in the band basis and their relation to each other. In Sec. III, we discuss how we can use a combination of the Wigner and Green functions for a complete model of the system. The Green functions will be used to model the off-diagonal elements (which are related to polarizations), and the Wigner functions will be used to model the diagonal elements (which are related to carrier densities). In Sec. IV, we describe the evolution equations of these two functions and explicitly specify self-energies for two main interactions: electromagnetic and first-order Coulombic. We also show the simplification of the various functions to the steady-state and their relation to susceptibility. In Sec. V, we present a sample calculation of the gain for a single quantum well (QW) laser using the developed formalism. This gives us a nonequilibrium correction term that is incorporated in standard formulations of gain. Finally, Sec. VI and VII present results and concluding remarks.

II. GREEN AND WIGNER FUNCTIONS

A. Real-time Green functions in position space

In the real-time approach to nonequilibrium Green functions on a Keldysh contour, six Green functions are defined.[10,17] They are the advanced G^a, retarded G^r, time-ordered G^t, antitime-ordered $G^{\bar{t}}$, and $G^<$ and $G^>$ (which are sometimes referred to as having no name[17] but otherwise called the lesser and greater Green functions,[18] respectively). The Green functions are defined in the standard way such as[10,17] $G^<(x_1,x_2)=\frac{i}{\hbar}\langle\hat{\psi}^+(x_2)\hat{\psi}(x_1)\rangle$, where $(\hat{\psi}^+(x_2))$ and $\hat{\psi}(x_1)$ are the field creation and annihilation operators with position and time coordinates $x_i=(\mathbf{r}_i,t_i)$. We will also use the matrix representation of Craig,[1,17,20]

$$\tilde{G}(x_1,x_2)=\begin{bmatrix} G^t(x_1,x_2) & -G^<(x_1,x_2) \\ G^>(x_1,x_2) & -G^{\bar{t}}(x_1,x_2) \end{bmatrix}. \quad (1)$$

B. Green functions in the eigenfunction basis

The field creation and annihilation operators are expanded into the eigenfunction basis,

$$\hat{\psi}^{+}(x) = \sum_{\alpha} \psi_{\alpha}^{*}(\mathbf{r})\hat{a}_{\alpha}^{+}(t), \quad \hat{\psi}(x) = \sum_{\alpha} \psi_{\alpha}(\mathbf{r})\hat{a}_{\alpha}(t), \tag{2}$$

where $H_0(\mathbf{r})\psi_\alpha(\mathbf{r})=\varepsilon_\alpha\psi_\alpha(\mathbf{r})$, and ψ_α and ε_α below are the eigenfunctions and eigenenergies, respectively, of the *noninteracting Hamiltonian*. The terms $\hat{a}_\alpha^+(t)/\hat{a}_\alpha(t)$ are the creation or annihilation operators for an electron in this state. We will discuss the meaning of eigenvalue index α later when we examine a specific model.

The Green functions can then be expanded into the eigenfunction basis as

$$G^{\gamma}(x_1,x_2) = \sum_{\alpha_1,\alpha_2} \psi_{\alpha_1}(\mathbf{r}_1)\psi_{\alpha_2}^{*}(\mathbf{r}_2)G^{\gamma}(\alpha_1,t_1,\alpha_2,t_2), \tag{3}$$

where γ represents all the different types of Green functions and $G^\gamma(\alpha_1,t_1,\alpha_2,t_2)$ is the Green function in the eigenfunction basis. We use in this and the next section the center of mass coordinates which are defined for time and position by

$$x = (x_1 + x_2)/2, \quad x_d = (x_1 - x_2) \rightarrow x_1 = x + x_d/2,$$

$$x_2 = x - x_d/2, \tag{4}$$

where $x=\{\mathbf{r},t\}$ and $x_d=\{\mathbf{r}_d,t_d\}$. The Green function in time-frequency coordinates is

$$\tilde{G}(\alpha_1,\alpha_2,t,\omega) = \int dt_d e^{i\omega t_d}\tilde{G}(\alpha_1,\alpha_2,t,t_d). \tag{5}$$

Later, we will generally use the Markovian approximation of the above function which is[10,17] $\tilde{G}(\alpha_1,\alpha_2,t) \equiv \int (d\omega/2\pi)\tilde{G}(\alpha_1,\alpha_2,t,\omega)$.

C. Wigner functions in the band basis

The second representation is in terms of the Wigner functions. First, write the Green functions in the band basis. It is a known fact that several bands exist in the vicinity of any symmetry point in semiconductors. We label those bands using index i and introduce $\hat{\psi}_i^+/\hat{\psi}_i$ as the field creation or annihilation operators for an electron in band i (conduction or valence).

The field creation and annihilation operators in the band basis are

$$\hat{\psi}^{+}(x) = \sum_{i} u_i^{*}(\mathbf{r})\hat{\psi}_i^{+}(x) \quad \text{and} \quad \hat{\psi}(x) = \sum_{i} u_i(\mathbf{r})\hat{\psi}_i(x), \tag{6}$$

where $u_i(\mathbf{r})$ is a normalized function periodic in the unit cell. The Green functions can then be written in this basis as

$$G^{\gamma}(x_1,x_2) = \sum_{i,j} u_i(\mathbf{r}_1)u_j^{*}(\mathbf{r}_2)G_{i,j}^{\gamma}(x_1,x_2), \tag{7}$$

where $G_{i,j}^{\gamma}(x_1,x_2)$ are the Green functions in the band basis. Note that the Green functions in the band basis still have a position dependence, but they are slowly varying with respect to the unit cell size. Finally, the Wigner-Weyl transformation on the function converts these to Wigner functions (in the Markovian approximation),[10,17]

$$f_{i,j}(\mathbf{r},\mathbf{k},t) = \int \frac{d\omega}{2\pi} d^4x_d e^{i\omega t_d - i\mathbf{k}\cdot\mathbf{r}_d} G_{i,j}^{<}(\mathbf{r},\mathbf{r}_d,t,t_d)$$

$$= \int d^3\mathbf{r}_d e^{-i\mathbf{k}\cdot\mathbf{r}_d} G_{i,j}^{<}(\mathbf{r},\mathbf{r}_d,t,0). \tag{8}$$

This function is defined in what will be called the *Wigner coordinates*, which correspond to phase space in the classical limit.

D. Relation between the Green functions in the eigenfunction basis and the Wigner functions

Since we will be using both Wigner and Green function representations in our model, we will need a method to convert between the two. Assume that the eigenfunctions of the noninteracting Hamiltonian can be expanded in the band basis as

$$\psi_\alpha(\mathbf{r}) = \sum_i F_{\alpha,i}(\mathbf{r})u_i(\mathbf{r}), \tag{9}$$

where $F_{\alpha,i}(\mathbf{r})$ are the envelope functions[13] and $u_i(\mathbf{r})$ are, again, fast varying functions. Substituting this relation into Eq. (3), and then equating Eq. (7) to Eq. (3) gives

$$\sum_{i,j} u_i(\mathbf{r}_1)u_j^{*}(\mathbf{r}_2)\tilde{G}_{i,j}(x_1,x_2)$$

$$= \sum_{i,j,\alpha_1,\alpha_2} u_i(\mathbf{r}_1)u_j^{*}(\mathbf{r}_2)F_{\alpha_1,i}(\mathbf{r}_1)F_{\alpha_2,j}^{*}(\mathbf{r}_2)\tilde{G}(\alpha_1,t_1,\alpha_2,t_2). \tag{10}$$

Since the above relation must hold for all functions $u_i(\mathbf{r})$, one can show the relationship

$$f_{i,j}(\mathbf{r},\mathbf{k},t) = \sum_{\alpha_1,\alpha_2} J_{\alpha_2,j}^{\alpha_1,i}(\mathbf{r},\mathbf{k})G^{<}(\alpha_1,\alpha_2,t), \tag{11}$$

with

$$J_{\alpha_2,j}^{\alpha_1,i}(\mathbf{r},\mathbf{k}) = \int d^3\mathbf{r}_d e^{-i\mathbf{k}\cdot\mathbf{r}_d} F_{\alpha_1,i}(\mathbf{r}+\mathbf{r}_d/2)F_{\alpha_2,j}^{*}(\mathbf{r}-\mathbf{r}_d/2). \tag{12}$$

The converse relationship can also be derived,

$$G^{<}(\alpha_1,\alpha_2,t) = \sum_{i,j} \frac{1}{(2\pi)^3} \int d^3\mathbf{k} d^3\mathbf{r} J^{*\alpha_1,i}_{\alpha_2,j}(\mathbf{r},\mathbf{k}) f_{i,j}(\mathbf{r},\mathbf{k},t). \tag{13}$$

Equations (11) and (13) give us conversion formulas between the two representations.

III. CHOOSING A COMPLETE SET OF FUNCTIONS FOR THE SYSTEM

Either representation presented so far could be used to completely describe the system. However, we can also use a combination of these two representations for a complete description. We will use the Green functions in the eigenfunction basis to describe interband correlations (which are re-

TABLE I. Summary of Green and Wigner functions used in the model.

Functions to solve
$G^{<,ch}(\alpha_{c_1},\alpha_{h_2})$: off-diagonal Green functions in the eigenfunction basis.
$f^{c}_{i_c,j_c}(\mathbf{r},\mathbf{k},t)$: diagonal Wigner functions for the conduction electrons in the band basis.
$f^{h}_{i_h,j_h}(\mathbf{r},\mathbf{k},t)$: diagonal Wigner functions for the holes in the band basis.
Intermediate functions
$f^{ch}_{i_c,j_h}(\mathbf{r},\mathbf{k},t)$: off-diagonal Wigner functions in the band basis.
$G^{<,c}(\alpha_{c_1},\alpha_{c_2},t)$: diagonal Green functions for the conduction electrons in the eigenfunction basis.
$G^{<,h}(\alpha_{h_1},\alpha_{h_2},t)$: diagonal Green functions for the holes in the eigenfunction basis.

lated to polarizations) and the Wigner functions in the band basis to describe intraband correlations (which are related to density functions).

Consider the wave functions in the system $\psi_\alpha(\mathbf{r})=\Sigma_i F_{\alpha,i}(\mathbf{r})u_i(\mathbf{r})$. In this function, the index i represents the subband index and α represents the eigenlevel. We now assume that the function $F_{\alpha,i}(\mathbf{r})$ is non-negligable only when α and i refer to the same band, that is, if i denotes a conduction subband and α refers to a state energetically in the conduction band (and similarly for the valence band). Looking at Eq. (12) for $J^{\alpha_1,i}_{\alpha_2,j}(\mathbf{r},\mathbf{k})$, with the above approximation in mind, implies that α_1 and i must represent the same bands and α_2 and j must also represent the same bands. Therefore, $f_{i,j}$ and $G^{<}(\alpha_1,\alpha_2)$ must describe functions in the same bands. This allows us to construct a complete solution to the system where the Wigner functions will only be used for "diagonal" states (cases where i and j are both in the same band) and the Green functions in the eigenfunction basis will only be used for "off-diagonal" functions (cases where α_1 and α_2 are in different bands).

We show in Table I our list of Green and Wigner functions. We have broken it into two groups. The first group are the functions we will solve with our evolution equations. They represent a complete set of states. In the second group are intermediate functions that can be found from the first group using the relations of Eqs. (11) and (13).

The $<$ superscript on the Green functions will hereafter be dropped.

We do not really need the intermediate functions; we could write the equations completely in terms of the first set of functions. However, for clarity, it is sometimes convenient to use them. When possible, we will put subscripts on the eigenlevels and band indices to indicate which band we are dealing with (such as α_c or α_h and i_c or i_h). Also, we use the hole representation for the valence band. The diagonal hole functions are related to the valence electron functions by $G^v(\alpha,\beta,t)=\delta_{\alpha,\beta}-G^h(\alpha,\beta,t)$ for the Green functions and $f^h_{i,j}(\mathbf{r},\mathbf{k},t)=\delta_{i,j}-f^v_{i,j}(\mathbf{r},\mathbf{k},t)$ for the Wigner functions. The off-diagonal functions will be the unchanged ones in the hole basis ($f^{cv}=f^{ch}$), except the implicit change in the momentum of the eigenlevels that goes along with this ($\mathbf{k}\rightarrow-\mathbf{k}$).

IV. EVOLUTION EQUATIONS FOR THE GREEN AND WIGNER FUNCTIONS

Now that we have the Green and Wigner functions and the relationship between them, we will describe their evolution. The evolution equations for both types of functions originate with the general Dyson's equations. In Dyson's equations, all interactions can be incorporated by the *self-energies*.[14,17,21] There are various ways to express Dyson's equations.[17,19] The form of interest here is shown below

$$\left[i\hbar\left(\frac{\partial}{\partial t_1}+\frac{\partial}{\partial t_2}\right)-(H_0(\mathbf{r}_1)-H_0(\mathbf{r}_2))\right]\tilde{G}(x_1,x_2)$$
$$=\sum_{EM,HF}\hbar\int dx_3[\tilde{\Sigma}^{EM,HF}(x_1,x_3)\tilde{G}(x_3,x_2)$$
$$-\tilde{G}(x_1,x_3)\tilde{\Sigma}^{EM,HF}(x_3,x_2)]+i\hbar$$
$$\times\left(\frac{\partial}{\partial t_1}+\frac{\partial}{\partial t_2}\right)\tilde{G}(x_1,x_2)\Big|_{scatt}, \tag{14}$$

where H_0 is the noninteracting part of the Hamiltonian which contains the kinetic energy and heterostructure potential energy (including electrostatic self-consistency and applied bias). This is the Hamiltonian that is diagonalized for the eigenfunctions used in the eigenfunction basis. The index EM,HF signifies the sum over the classical electromagnetic and first-order Coulombic (Hartree-Fock) interactions. We have also considered phonon and higher-order Coulombic interactions[1,22] which will lead to scattering terms, to be discussed below. Here, they are represented formally as $\left(\frac{\partial}{\partial t_1}+\frac{\partial}{\partial t_2}\right)\tilde{G}(x_1,x_2)|_{scatt}$.

A. EM and HF self-energies

The classical EM self-energy in general position space can be written as[9]

$$\tilde{\Sigma}^{EM}(x_1,x_2)=-\frac{e}{\hbar}\tilde{I}\delta^4(x_1-x_2)\mathbf{E}(\mathbf{r}_1,t_1)\cdot\mathbf{r}_1, \tag{15}$$

where $\tilde{I}$ is the identity matrix in Craig's space and $\mathbf{E}$ is the classical electric field. The HF self-energy is the first-order Coulombic terms. The only nonzero terms are the time-ordered and antitime-ordered ones which can be shown to be (most conveniently in eigenfunction space)[14,22,23]

$$\Sigma^{HF,t/\bar{t}}(\alpha_1,\alpha_2,t)=\frac{i}{\hbar}\sum_{\alpha_1',\alpha_2'}G^{t/\bar{t}}(\alpha_1',\alpha_2',t)V_s(\alpha_1,\alpha_1',\alpha_2,\alpha_2'), \tag{16}$$

where

$$V_s(\alpha_1,\alpha_1',\alpha_2,\alpha_2') = \int d^3\mathbf{r}_1 d^3\mathbf{r}_2 V_s \times(|\mathbf{r}_1-\mathbf{r}_2|)\psi^*_{\alpha_1}(\mathbf{r}_1)\psi_{\alpha_1'}(\mathbf{r}_1)\psi_{\alpha_2}(\mathbf{r}_2)\psi^*_{\alpha_2'}(\mathbf{r}_2) \tag{17}$$

and $V_s(|\mathbf{r}|)$ is a renormalized potential to account for screening, which could be given by, for example, the plasmon-pole approximation.[12] These self-energies must be transformed into the eigenfunction basis and the Wigner coordinates in the band basis for use in the evolution equations.

B. Higher-order scattering

The scattering terms due to phonon and second order Coulombic interactions have been derived in both the eigenfunction basis[14] and Wigner space.[1,24] While there are some additional complications, in principle, there is no reason why they could not also be incorporated here.[22] However, due to the large increases in computation time which these terms bring about and which do not affect the purpose of this article, we will adopt the commonly used rate equation approximation for them.

Green functions in this approximation take the form[25]

$$\left.\frac{\partial G^{ch}(\alpha_c,\alpha_h,t)}{\partial t}\right|_{scatt} = \gamma_{\alpha_c,\alpha_h}(G_o^{ch,eq}(\alpha_c,\alpha_h) - G^{ch}(\alpha_c,\alpha_h,t)), \tag{18}$$

and for the Wigner functions, this is[7,12,24,25]

$$\left.\frac{\partial f_{i,j}^{c/h}(\mathbf{r},\mathbf{k},t)}{\partial t}\right|_{scatt} = \gamma_{ij}[f_{o,i,j}^{c/h,eq}(\mathbf{r},\mathbf{k}) - f_{i,j}^{c/h}(\mathbf{r},\mathbf{k},t)], \tag{19}$$

where $G_o^{ch,eq}$ and $f_o^{c/h,eq}$ are equilibrium Green and Wigner functions, respectively. The Green function scattering can be simplified because, in equilibium, there are no off-diagonal components ($G_o^{ch,eq}=0$).[12] The symbol $\gamma_{i,j}$ is the relaxation rate for the Wigner functions, and $\gamma_{\alpha_c,\alpha_h}$ is the relaxation rate of the Green functions. In general, these rates will be dependent on energy or momentum as they come from the collision integrals of the scattering processes.[24] For simplicity, we will approximate them as constant. A simple extension to this approximation is to add scattering terms for each type of interaction.[25]

C. Rotating wave approximation

The rotating wave approximation is a common technique used to separate the quickly and slowly varying components of functions with time dependence.[12,14] We assume that any function of time can be written as

$$f(t) \approx \tilde{f}(t)e^{-\Omega_{op}T} + \tilde{f}^*(t)e^{-\Omega_{op}T} \tag{20}$$

for a device operating around a single optical frequency Ω_{op}. This replacement is done for any time-varying function in the evolution equations. The evolution equations are then multiplied by $\int_{t-\tau}^{t+\tau} dt'$ where $\tau=\frac{2\pi}{\Omega_{op}}$. The slowly varying components have a negligible change over this time, while any components with terms of $e^{n\Omega_{op}T}$, $n=\pm1,\pm2,\ldots$, will average to zero. Thus, we will end up with equations that are only slowly varying in time.

D. Evolution of the off-diagonal Green functions in the eigenfunction basis

Substitute the EM and HF self-energies into Eq. (14), transform to the eigenfunction basis, and use the Boltzmann scattering and rotating wave approximations to get the off-diagonal functions[12,14,22,25]

$$\begin{aligned}\sum_{\alpha_c',\alpha_h'}&\left[\hbar\left(i\frac{\partial}{\partial t}+\Omega_{op}+i\gamma_{\alpha_c,\alpha_h}\right)\delta_{\alpha_c,\alpha_c'}\delta_{\alpha_h,\alpha_h'} - (\mathcal{E}^{c,\alpha_c,\alpha_h}_{\alpha_c',\alpha_h'}(t) - \mathcal{E}^{h,\alpha_c,\alpha_h}_{\alpha_c',\alpha_h'}(t)) + V_s(\alpha_c,\alpha_c',\alpha_h,\alpha_h')\right]G^{ch}(\alpha_c',\alpha_h',t)\\ &= -i\sum_{i_c,j_h}\mathbf{d}_{i_c,j_h}\cdot\mathbf{E}^+(t)\left[I^{\alpha_c,i_c}_{\alpha_h,j_h} - \sum_{\beta_h} I^{\alpha_c,i_c}_{\beta_h,j_h}G^h(\beta_h,\alpha_h,t) - \sum_{\beta_c} I^{\beta_c,i_c}_{\alpha_h,j_h}G^c(\alpha_c,\beta_c,t)\right],\end{aligned} \tag{21}$$

where

$$\begin{aligned}\mathcal{E}^{c,\alpha_c,\alpha_h}_{\alpha_c',\alpha_h'}(t) &= \left(\varepsilon^c_{\alpha_c}\delta_{\alpha_c,\alpha_c'} + \sum_{\beta_c,\beta_c'} G^c(\beta_c,\beta_c',t)V_s(\alpha_c,\beta_c,\alpha_c',\beta_c')\right)\delta_{\alpha_h,\alpha_h'}\\ &\quad + \sum_{\beta_c} V_s(\beta_c,\alpha_c',\alpha_h,\alpha_h')G^c(\alpha_c,\beta_c,t)\end{aligned} \tag{22}$$

and

$$\begin{aligned}\mathcal{E}^{h,\alpha_c,\alpha_h}_{\alpha_c',\alpha_h'}(t) = \Bigg(&\varepsilon^h_{\alpha_h}\delta_{\alpha_h,\alpha_h'} + \sum_{\beta_h,\beta_h'} V_s(\alpha_h',\beta_h,\alpha_h,\beta_h')(G^h(\beta_h,\beta_h',t) - \delta_{\beta_h,\beta_h'})\Bigg)\delta_{\alpha_c,\alpha_c'} - \sum_{\beta_h} V_s(\alpha_c,\alpha_c',\beta_h,\alpha_h')G^h(\beta_h,\alpha_h,t)\end{aligned} \tag{23}$$

are the HF renormalized energies, $I^{\alpha_1,i_1}_{\alpha_2,i_2} = \int d^3\mathbf{r} F^*_{\alpha_1,i_1}(\mathbf{r})F_{\alpha_2,i_2}(\mathbf{r})$ is the overlap intergral, and $\mathbf{d}_{ij} = e\int d^3\mathbf{r} u_i^*(\mathbf{r})u_j(\mathbf{r})\mathbf{r}$ is the interband polarization. The noninteracting Hamiltonian terms have been replaced by their eigenvalues $\varepsilon^{h/c}_{\alpha}$.

E. Evolution of the diagonal Wigner functions in the band basis

We begin once again with Dyson's equations and transform them to the band basis. Expanding the position space Green functions and self-energies in Eq. (14) into the band basis, multiplying the resulting equation by $\int_\Omega d^3\mathbf{r}_1 d^3\mathbf{r}_2 u_i^*(\mathbf{r}_1)u_j(\mathbf{r}_2)$ (where the Ω subscript on the integral denotes only integrating over the volume of the unit cell) and transforming into the Wigner coordinates give[1,7,9,16,17]

$$i\hbar\frac{\partial}{\partial t}f^{c}_{i_c,j_c}(\mathbf{r},\mathbf{k},t)+\sum_{i'}\int d^3\mathbf{k}'[\mathcal{H}^{(+,c)}_{i_c,i'}(\mathbf{r},\mathbf{k},\mathbf{k}',t)f^{c}_{i',j_c}(\mathbf{r},\mathbf{k}',t)-\mathcal{H}^{(-,c)}_{i',j_c}(\mathbf{r},\mathbf{k},\mathbf{k}',t)f^{c}_{i_c,i'}(\mathbf{r},\mathbf{k}',t)]$$

$$=-\sum_{i_h}\int d^3\mathbf{k}'[\{V_s(\mathbf{k}-\mathbf{k}')f^{hc}_{i_h,j_c}(\mathbf{r},\mathbf{k}',t)+\mathbf{d}_{i_h,i_c}\cdot\mathbf{E}^{-}(\mathbf{r},t)\}f^{ch}_{i_c,i_h}(\mathbf{r},\mathbf{k},t)-\{V_s(\mathbf{k}-\mathbf{k}')f^{ch}_{i_c,i_h}(\mathbf{r},\mathbf{k}',t)+\mathbf{d}_{i_c,i_h}\cdot\mathbf{E}^{+}(\mathbf{r},t)\}f^{hc}_{i_h,j_c}(\mathbf{r},\mathbf{k},t)]$$

$$+i\hbar\gamma_{i_c,j_c}[f^{c,eq}_{o,i_c,j_c}(\mathbf{r},\mathbf{k})-f^{c}_{i_c,j_c}(\mathbf{r},\mathbf{k},t)], \tag{24}$$

and the equation for the holes is the same, except for all c/h indices being switched. The HF renormalized Hamiltonian terms are $\mathcal{H}^{(\pm,\gamma)}_{i,j}(\mathbf{r},\mathbf{k},\mathbf{k}',t)=H^{(\pm,\gamma)}_{i,j}(\mathbf{r},\mathbf{k},\mathbf{k}')+V_s(\mathbf{k}-\mathbf{k}')\times f^{\gamma}_{i,j}(\mathbf{r},\mathbf{k},t)$, with $H^{+}_{i,j}(\mathbf{r},\mathbf{k},\mathbf{k}')$ and $H^{-}_{i,j}(\mathbf{r},\mathbf{k},\mathbf{k}')$ being $H_{0,i,j}(\mathbf{r}_1)$ and $H_{0,i,j}(\mathbf{r}_2)$ transformed into the Wigner coordinates, respectively. The terms $H_{0,i,j}(\mathbf{r}_1)=\int_\Omega d^3\mathbf{r}u^{*}_i(\mathbf{r})H_0(\mathbf{r})u_j(\mathbf{r})$ are the noninteracting Hamiltonian terms in the band basis. The superscript γ denotes the band (C, HH, LH). We show these terms for the parabolic model in Eq. (38). The symbol E^{+} is the positive frequency component of the electric field in the rotating wave approximation.[24] We also have Coulombic terms $V_s(|k-k'|)=\frac{1}{(2\pi)^3}\int d^3\mathbf{r}_d e^{-i(\mathbf{k}-\mathbf{k}')\cdot\mathbf{r}_d}V_s(|r_d|)$ in the HF renormalized terms.

Equations (21) and (24) represent our solution for the time-dependent case. If we had an expression for the electric field, we would have a self-consistent solution. These would be an appropriate set of equations to use for analysis of a time-transient system. We will now look at the steady-state solution.

F. Steady-state case: Susceptibility and the self-consistent solution

In the $t\to\infty$ limit and with the rotating wave approximation, all the time-dependent functions approach their steady-state solutions. To express this using our equations, all t dependence will be removed and any time derivative will vanish. The steady-state off-diagonal Green function is then

$$G^{ch}(\alpha_c,\alpha_h)=-\mathbf{T}_{\alpha_c,\alpha_h}\cdot\mathbf{E}^{+}, \tag{25}$$

with

$$\mathbf{T}_{\alpha_c,\alpha_h}=\sum_{i_c,j_h,\alpha'_c,\alpha'_h}\mathbf{d}_{i_c,j_h}\frac{\left[I^{\alpha'_c,i_c}_{\alpha'_h,j_h}-\sum_{\beta_h}I^{\alpha'_c,i_c}_{\beta_h,j_h}G^{h}(\beta_h,\alpha'_h)-\sum_{\beta_c}I^{\beta_c,i_c}_{\alpha'_h,j_h}G^{c}(\alpha'_c,\beta_c)\right]}{[\hbar(\Omega_{op}+i\gamma_{\alpha_c,\alpha_h})\delta_{\alpha_c,\alpha'_c}\delta_{\alpha_h,\alpha'_h}-(\mathcal{E}^{c,\alpha'_c,\alpha'_h}_{\alpha_c,\alpha_h}-\mathcal{E}^{h,\alpha'_c,\alpha'_h}_{\alpha_c,\alpha_h})+V_s(\alpha'_c,\alpha_c,\alpha'_h,\alpha_h)]}. \tag{26}$$

In the rotating wave approximation, the relation between the macroscopic polarization density and Green functions is

$$\mathbf{P}^{+}(\mathbf{r})=i\sum_{\alpha_c,\alpha_h,i_c,j_h}\mathbf{d}^{*}_{i_c,j_h}F_{\alpha_c,i_c}(\mathbf{r})F^{*}_{\alpha_h,j_h}(\mathbf{r})G^{ch}(\alpha_c,\alpha_h)$$

$$=-i\sum_{\alpha_c,\alpha_h,i_c,j_h}F_{\alpha_c,i_c}(\mathbf{r})F^{*}_{\alpha_h,j_h}(\mathbf{r})\mathbf{d}^{*}_{i_c,j_h}\mathbf{T}_{\alpha_c,\alpha_h}\cdot\mathbf{E}^{+}(\mathbf{r}). \tag{27}$$

Electric susceptibility is defined as[13]

$$\mathbf{P}(\mathbf{r})=\bar{\bar{\chi}}_{c,h}(\mathbf{r})\cdot\mathbf{E}(\mathbf{r}), \tag{28}$$

where $\bar{\bar{\chi}}_{c,h}$ is the complex susceptibility which has a dyadic dependence in the polarization directions.

Equating Eq. (28) to Eq. (27) defines the complex susceptibility as

$$\chi^{\beta}_{c,h}(\mathbf{r})=-i\sum_{\alpha_c,\alpha_h,i_c,j_h}F_{\alpha_c,i_c}(\mathbf{r})F^{*}_{\alpha_h,j_h}(\mathbf{r})d^{\beta*}_{i_c,j_h}T^{\gamma}_{\alpha_c,\alpha_h}. \tag{29}$$

Here, β defines the polarization direction, and only the induced polarization that has the same direction as the electric field is considered. The real and complex parts define a position dependent refractive index and gain $n^{\beta}_{c,h}(\mathbf{r},t)=\mathrm{Re}\,\chi^{\beta}_{c,h}(\mathbf{r},t)$, $g^{\beta}_{c,h}(\mathbf{r},t)=\mathrm{Im}\,\chi^{\beta}_{c,h}(\mathbf{r},t)$.

For the diagonal Wigner functions, Eq. (24) can then be written as

$$\sum_{i'} \int d^3\mathbf{k}'[\mathcal{H}^{(+,c)}_{i_c,i'}(\mathbf{r},\mathbf{k},\mathbf{k}')f^c_{i',j_c}(\mathbf{r},\mathbf{k}') - \mathcal{H}^{(-,c)}_{i',j_c}(\mathbf{r},\mathbf{k},\mathbf{k}')f^c_{i_c,i'}(\mathbf{r},\mathbf{k}')]$$

$$= \frac{|E|^2}{2}\sum_{i_h} \int d^3\mathbf{k}'[(V_s(\mathbf{k}-\mathbf{k}')T^{\beta*}_{j_c,i_h}(\mathbf{r},-\mathbf{k}') + d^{\beta}_{i_h,i_c})T^{\beta}_{i_c,i_h}(\mathbf{r},\mathbf{k}) - (V_s(\mathbf{k}-\mathbf{k}')T^{\beta}_{i_c,i_h}(\mathbf{r},\mathbf{k}') + d^{\beta}_{i_c,i_h})T^{\beta*}_{j_c,i_h}(\mathbf{r},-\mathbf{k})]$$

$$+ i\hbar\gamma_{i_c,j_c}[f^{c,eq}_{o,i_c,j_c}(\mathbf{r},\mathbf{k}) - f^c_{i_c,j_c}(\mathbf{r},\mathbf{k})], \tag{30}$$

with $\mathbf{T}_{i_c,j_h}(\mathbf{r},\mathbf{k}) = -\Sigma_{\alpha_c,\alpha_h} J^{\alpha_c,i_c}_{\alpha_h,j_h}(\mathbf{r},\mathbf{k})\mathbf{T}_{\alpha_c,\alpha_h}$. A similar relation exists for holes.

Equation (30) with Eqs. (25) and (29) represent the final solution to our steady-state model. Combining these with a relation for the magnitude of the electric field will give a fully self-consistent set of equations for the magnitude of the electric field (which can be related to power), gain, and carrier densities. Relations for the electric field terms $|E|^2$ will not be discussed here, but one possibility is to use a Langevin model for spontaneous emission which will give the field in terms of the susceptibility and diffusion coefficient[22,26,27] and the electromagnetic Green functions for the dielectric cavity type (for example, Fabry-Perot or distributed feedback).

V. EXAMPLE: CALCULATING THE GAIN OF A QUANTUM WELL LASER

Up to this point, the model has been quite general in both device and band structure approximations. The only requirement is that the eigenfunctions can be separated into a slowly varying function multiplied by a fast varying function with respect to the lattice constant. This can be applied for parabolic, Luttinger-Kohn (LK), and tight-binding models. In this section we will look at a simple QW laser grown in the z direction.

We begin by making three key simplifying approximations:

(1) In Eqs. (21) and (24), the Coulombic energy renormalization effects are incorporated in $\mathcal{E}$ and $\mathcal{H}$. For example, these terms will be simplified by adopting a common approximation where the energy renormalization is simply added to the band's potential $V_\gamma(z)$ (Refs. 12 and 28) of the form $\Delta E_\gamma(n) = \beta_\gamma n^{1/3}_\gamma(z)$. The symbol β_γ is known as the band-gap shrinkage coefficient of this band (including band offset), and the symbol $n_\gamma(z)$ is the carrier density which will change for each iteration.

(2) Assume negligible intraband off-diagonal elements due to high intraband scattering rates. This means any diagonal Wigner or Green functions will be reduced to $G^\gamma(\alpha_1,\alpha_2) = \delta_{\alpha_1,\alpha_2}G^\gamma(\alpha_1,\alpha_1) \equiv G^\gamma(\alpha_1)$ and $f^\gamma_{i,j}(\mathbf{r},\mathbf{k}) = \delta_{i,j}f^\gamma_{i,i}(\mathbf{r},\mathbf{k}) \equiv f^\gamma_i(\mathbf{r},\mathbf{k})$.

(3) Assume that the electric field coupling terms are negligible in the diagonal Wigner function equations. Thus, any terms with $|E|^2$ will be removed.

A. Mixed LK and parabolic approximation

Ideally, we would like to solve both the Green functions and Wigner functions using the same band structure (in this case, LK) model. However, the large number of bands of the LK model significantly increases the computation time for the Wigner functions. At the same time, the parabolic model is insufficient for accurate calculations for gain. We therefore adopt the compromise presented below.

First, note that in the LK and parabolic approximations, the envelope functions are

$$F_{\alpha,i}(\mathbf{r}) = F_{n_h,\mathbf{q}_h,i}(\mathbf{r}) = F_{n_h,\mathbf{q}_h,i}(z)\frac{e^{i\mathbf{q}_h\cdot\mathbf{r}_\perp}}{2\pi} \tag{31}$$

for 4×4 LK holes and

$$F_{\alpha,i}(\mathbf{r}) = F_{n_\gamma,\mathbf{q}_\gamma i}(\mathbf{r}) = \delta_{i,i_{n_\gamma}}F_{n_\gamma,i}(z)\frac{e^{i\mathbf{q}_\gamma\cdot\mathbf{r}_\perp}}{(2\pi)} \tag{32}$$

for parabolic electrons and holes. Here, i_{n_γ} denotes the subband this level is in (which is possible because there is no band mixing in this case). The eigenstates α used throughout this work will be of the form $\alpha_\gamma = \{n_\gamma,\mathbf{q}_\gamma\}$, where n_γ is the band-edge eigenlevel and $\mathbf{q}_\gamma$ is the transverse momentum, not to be confused with the momentum indices in the Wigner functions which will use $\mathbf{k}$.

With the eigenlevels in this form above, write the (intermediate, diagonal) Green functions as the sum of two components, the best-fit equilibrium component, which will be a Fermi function, and the nonequilibrium correction term

$$G^\gamma_{\mathrm{LK}}(n_\gamma,\mathbf{q}) = G^{eq,\gamma}_{\mathrm{LK}}(n_\gamma,\mathbf{q}) + \delta G^\gamma_{\mathrm{LK}}(n_\gamma,\mathbf{q}) \tag{33}$$

and

$$G^\gamma_{parab}(n_\gamma,\mathbf{q}) = G^{eq,\gamma}_{parab}(n_\gamma,\mathbf{q}) + \delta G^\gamma_{parab}(n_\gamma,\mathbf{q}). \tag{34}$$

As will be discussed in more detail shortly, in the parabolic model, the equilibrium component is found by finding the best-fit Fermi distribution in the well region to the carrier distribution calculated from the Wigner function. The nonequilibrium correction term is then the difference between the calculated Wigner function and equilibrium component, transformed into the eigenfunction basis.

Our simplifying approximation is then to assume that the nonequilibrium correction term in the LK model is approximately equal to the nonequilibrium correction term in the parabolic model [$\delta G^\gamma_{\mathrm{LK}}(n_\gamma,\mathbf{q}) \approx \delta G^\gamma_{parab}(n_\gamma,\mathbf{q})$]. We also use

the Fermi levels found in the fitting procedure in the parabolic model for the LK model. The Green function in the LK model can then approximately be written as

$$G^{\gamma}_{\mathrm{LK}}(n_{\gamma},\mathbf{q}) \approx G^{eq,\gamma}_{\mathrm{LK}}(n_{\gamma},\mathbf{q}) + \delta G^{\gamma}_{parab}(n_{\gamma},\mathbf{q}). \tag{35}$$

With this approximation, we can use the LK model to calculate the optical gain and use the parabolic model to calculate a correction term due to the nonequilibrium nature of this system. The susceptibility of Eq. (29) therefore becomes

$$\chi^{\gamma}_{c,h} = -i\sum_{n_c,\mathbf{q},n_h} |\bar{I}^{n_c,\mathbf{q},i_c}_{n_h,\mathbf{q},j_h}|^2 |d^{\gamma *}_{i_c,j_h}|^2 \frac{[1-[G^{h,eq}_{\mathrm{LK}}(n_h,\mathbf{q})+\delta G^{h}_{parab}(n_h,\mathbf{q})]-[G^{c,eq}_{\mathrm{LK}}(n_c,\mathbf{q})+\delta G^{c}_{parab}(n_c,\mathbf{q})]]}{[\hbar(\Omega_{op}+i\gamma_{n_c,n_h})-(\varepsilon^{c}_{n_c,\mathbf{q}}-\varepsilon^{h}_{n_h,\mathbf{q}})]}, \tag{36}$$

where $\bar{I}^{n_1,\mathbf{q},i}_{n_2,\mathbf{q},j} = \int dz F^{*}_{n_1,\mathbf{q},i}(z) F_{n_2,\mathbf{q},j}(z)$. Equation (36) is very similar to standard formulations,[12,13,28] the difference being our nonequilibrium correction term.

The procedure is then as follows:

(1) Calculate the Wigner functions in the parabolic model.

(2) Find the equilibrium component and the nonequilibrium correction term to these Wigner functions.

(3) Assuming the Fermi level found in step 2 for the parabolic model will be close to what would be calculated with an LK model, use this to calculate $G^{eq,\gamma}_{\mathrm{LK}}(n_{\gamma},\mathbf{q})$.

(4) Use the equilibrium components and correction terms to calculate the susceptibility.

It is important to remember that this correction procedure is only necessary when we are using two different band-structure models for the diagonal and off-diagonal functions. This could also be used for higher-order models such as 4×4 LK for diagonal Wigner functions and 10×10 LK for off-diagonal Green functions. In the following, we provide the mathematical details for this procedure.

B. Equilibrium component and nonequilibrium correction term

To find the two components, we must first calculate the Wigner function in the parabolic model.

1. Diagonal Wigner functions: Parabolic approximation

The noninteracting Hamiltonians are a sum of the kinetic and potential energies, where the potentials included here are the heterostructure, applied bias, and electrostatic self-consistent energies. In the model used, the electrons and holes are uncoupled from each other so that the Hamiltonian can be separated into conduction and hole subblocks as

$$H^{\gamma}_{0,i,j}(\mathbf{r}) = \delta_{i,j}\left(\nabla_{\mathbf{r}}\cdot\frac{\hbar^2}{2m^{*}_{\gamma}(z)}\nabla_{\mathbf{r}} + V_{\gamma}(z)\right), \tag{37}$$

where γ are HH, LH, or C bands and i is the subband in this band. The effective mass is position dependent, and $V_{\gamma}(z)$ is the renormalized potential energy term for these bands.

The noninteracting part of the Hamiltonian in Wigner coordinates can be approximated as

$$H^{(\pm,\gamma)}_{i}(\mathbf{r},\mathbf{k},\mathbf{k}') \approx \delta(\mathbf{k}_{\perp}-\mathbf{k}'_{\perp}) H^{(\pm,\gamma)}_{i,i}(z,k_z,k'_z), \tag{38}$$

where

$$H^{(\pm,\gamma)}_{i}(z,k_z,k'_z) = \frac{e^{\pm 2i(k'_z-k_z)z}}{\pi}\left\{M^{\gamma}_{i}(\pm 2(k'_z-k_z))\left[\frac{1}{4}\partial^2_z \pm \frac{i}{2}\partial_z \times(k'_z+k_z) - k_z k'_z\right] + V^{\gamma}_{i}[\pm 2(k'_z-k_z)]\right\}. \tag{39}$$

The approximation in Eq. (38) comes from assuming that the derivative terms in the transverse direction are negligble compared to the other terms. The terms $V^{\gamma}(k_z)$ and $M^{\gamma}(k_z)$ are spatial Fourier transforms of $V^{\gamma}(\mathbf{r})$ and $\frac{\hbar^2}{2m^{*}_{\gamma}}(\mathbf{r})$, respectively, averaged over the transverse position and momentum directions.

Integrating Eq. (30) by $\int d^2\mathbf{r}_{\perp} d^2\mathbf{k}_{\perp}$ gives the quantum Boltzmann equation averaged over transverse direction and momentum.

$$\int dk'_z [H^{(+,\gamma)}_{i_{\gamma}}(z,k_z,k'_z) - H^{(-,\gamma)}_{i_{\gamma}}(z,k_z,k'_z)] f^{\gamma}_{i_{\gamma}}(z,k'_z) = i\hbar\gamma_{i_{\gamma}}[f^{\gamma,eq}_{o,i_{\gamma}}(z,k_z) - f^{\gamma}_{i_{\gamma}}(z,k_z)]. \tag{40}$$

2. Best-fit equilibrium component

The Fermi distribution in Wigner coordinates is

$$f^{\gamma,eq}_{i_{\gamma}}(z,k_z) = \sum_{n_{\gamma}} \bar{J}^{n_{\gamma},i_{\gamma}}(z,k_z) G^{\gamma,eq}(n_{\gamma},E^{\gamma}_{f}) \tag{41}$$

from the relation between the Wigner functions and the Green functions simplified from Eq. (11) and $\bar{J}^{n_{\gamma},i_{\gamma}}(z,k_z) = \int dz_p e^{-ik_z z_d} F_{n_{\gamma},i_{\gamma}}(z+z_d/2) F^{*}_{n_{\gamma},i_{\gamma}}(z-z_d/2)$. The function $G^{\gamma,eq}(n,E^{\gamma}_{f})$ is the Fermi function averaged over the transverse momentum $(\mathbf{q})$[13] and E^{γ}_{f} is the Fermi energy for this level. The procedure to find the best-fit equilibrium component is then to iterate guesses for E^{γ}_{f} to minimize the difference $|f^{\gamma}_{i}(z,k_z) - f^{\gamma,eq}_{i}(z,k_z)|$ within the well region. Once this is done, we use $G^{\gamma,eq}(n_{\gamma},E^{\gamma}_{f})$ as our best-fit equilibrium component.

3. Nonequilibrium correction term

Using the relation between the Green functions and the Wigner functions from Eq. (13), the nonequilibrium correction term can then be written as

$$\delta G^{\gamma}_{parab}(n_\gamma) = \frac{1}{2\pi}\int dk_z dz \bar{J}^{n_\gamma i_\gamma *}(z,k_z) f^{\gamma}_{i_\gamma}(z,k_z) - G^{\gamma,eq}_{parab}(n_\gamma, E^{\gamma}_f). \quad (42)$$

Finally, we want to use $\delta G^{\gamma}_{parab}(n_\gamma, \mathbf{q}, E^{\gamma}_f)$ (the correction term not averaged over the transverse momentum) in Eq. (36). We approximate this as $\delta G^{\gamma}_{parab}(n_\gamma, \mathbf{q}, E^{\gamma}_f) \approx \delta G^{\gamma}_{parab}(n_\gamma) K(n_\gamma, \mathbf{q}, E^{\gamma}_f)$, with $K(n_\gamma, \mathbf{q}, E^{\gamma}_f) = G^{\gamma,eq}_{parab} \times (n_\gamma, \mathbf{q}, E^{\gamma}_f) / G^{\gamma,eq}_{parab}(n_\gamma, E^{\gamma}_f)$. $K(n_\gamma, \mathbf{q}, E^{\gamma}_f)$ is a known quantity since we now know the Fermi level.

C. Boundary conditions

One of the main purposes of using Wigner functions is the ease of formulating boundary conditions and hence modeling an open system. The boundary conditions to use are at the ends of each structure (positions $z=0, L$), the carriers are approximately in equilibrium with Fermi levels μ_0 and μ_L,[7,9]

$$f^{\gamma}_{i_n}(z = 0/L, k_z) = \frac{m_n k_B T}{\pi\hbar^2} \ln[1 + e^{-(\varepsilon_{n,0/L} - \mu_{0/L})/k_B T}]. \quad (43)$$

D. Carrier capture

The Boltzmann scattering of Eq. (19) can be thought of as a carrier capture term where carriers are scattered into the well because we take the equilibrium functions $f^{\gamma,eq}_{i_\gamma}(z,k_z)$ to be Wigner functions for carriers in the well. These are approximated by assuming that the average electron and hole densities in the well are equal to the doping levels of boundary layers. Since they are in equilibrium, the carriers will redistribute themselves as a Fermi distribution,

$$f^{\gamma,eq}_{o,i_\gamma}(z,k_z) = \sum_{n_\gamma} \bar{J}_{n_\gamma i_\gamma}(z,k_z) G^{\gamma,eq,well}_{o}(n_\gamma), \quad (44)$$

where $G^{\gamma,eq,well}_{o}(n_\gamma)$ is a Fermi distribution (averaged over the transverse momentum) assuming all injected carriers in equilibrium and confined to the well. The carrier capture rates are generally in the range of 10/ps.

VI. RESULTS

We apply the above approximations to a single quantum well laser with the following structure as described in Table II. The numerical procedure to calculate the Wigner functions has been explained elsewhere.[7,9,11] We use a center-upwind finite difference method and solve self-consistently with Poisson's equation.

In Fig. 1, we show the self-consistent heterostructure potential for the electrons and holes using applied biases of 1.4 and 1.45 V. Because of self-consistency, the heterostructure potential in regions close to the well flattens. This is similar to what one would find using drift-diffusion methods. In standard gain calculations, it is often assumed that these potentials are flat to begin with.

TABLE II. Heterostructure of the quantum well laser modeled in the example.

Layer	Material	Width	Doping
1	InP	"Infinite"	$5\times10^{18}/\mathrm{cm}^3$, n type
2	InP	8 nm	None
3	$In_{0.53}Ga_{0.47}As$	6 nm	None
4	InP	8 nm	None
1	InP	"Infinite"	$5\times10^{18}/\mathrm{cm}^3$, p type

In Fig. 2, we show the total carrier density calculated from the Wigner functions, the best-fit equilibrium contribution, and the difference between these two. Only the HH and C bands are shown since the LH band concentrations are small. The difference, when transformed to the Green functions in the eigenfunction basis, becomes our previously mentioned nonequilibrium correction term. These are calculated with a capture rate $\gamma = 10/\mathrm{ps}$.

There are large conduction band carrier concentrations at the left boundary and large hole band carrier concentrations at the right boundary due to the doping of the boundary layers. As expected, there are also carrier accumulations in the well region. The conduction and hole densities in layers directly adjacent to the wells are dependent on the doping profile in the structure. The best-fit equilibrium contribution in the well is fairly close to the total carrier contribution there. The difference is relatively small and is mainly made up of higher-energy states. The gain will depend mainly on the lower-energy states.

In Fig. 3, we show the TE gain. To highlight the difference, we calculate the gain using our proposed equilibrium plus correction term as well as a naive approximation where we use all carriers localized around the well in the gain cal-

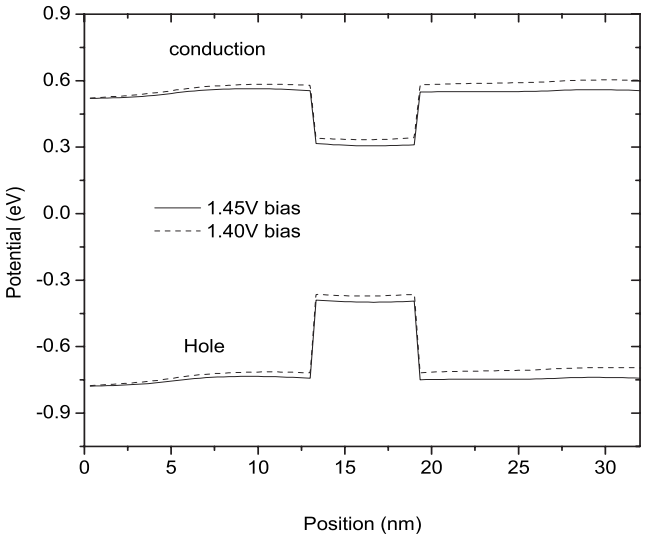

FIG. 1. Graph of self-consistent heterostructure potential for the electron and hole bands. It is shown for two bias voltages. Capture rate $\gamma = 10/\mathrm{ps}$.

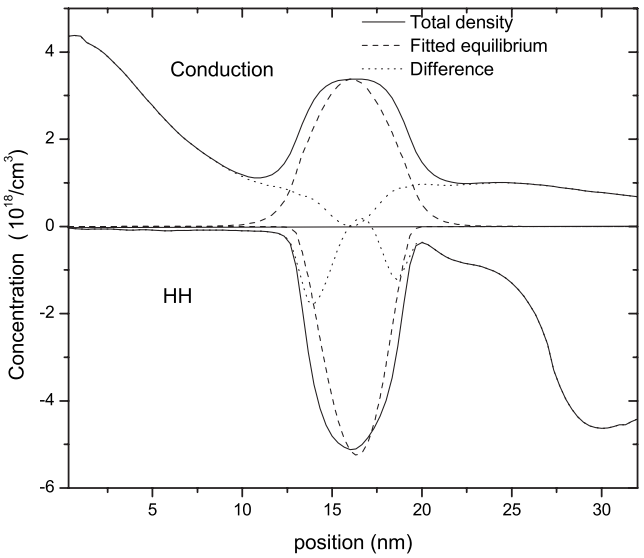

FIG. 2. Graph of carrier density for the electron and heavy hole bands. We show the total carrier density calculated from the Wigner functions, the best-fit equilibrium contribution, and the difference between these two. Capture rate $\gamma=10/\mathrm{ps}$.

culation (we imagine that the total carrier concentration is in equilibrium, find its Fermi level, and use that input for the gain equations). We see that using all carriers significantly overestimates the gain (in a sense, this is like using both the two-dimensional and three-dimensional carriers in a combined gain-rate equation model to calculate the gain).

One may ask if it is reasonable to just drop the correction term entirely and only use the best-fit equilibrium contribution. This is shown in Fig. 4 for a bias of 1.45 V and a capture rate of 10/ps. In this case, it will underestimate the actual gain, but it can also overestimate it depending on

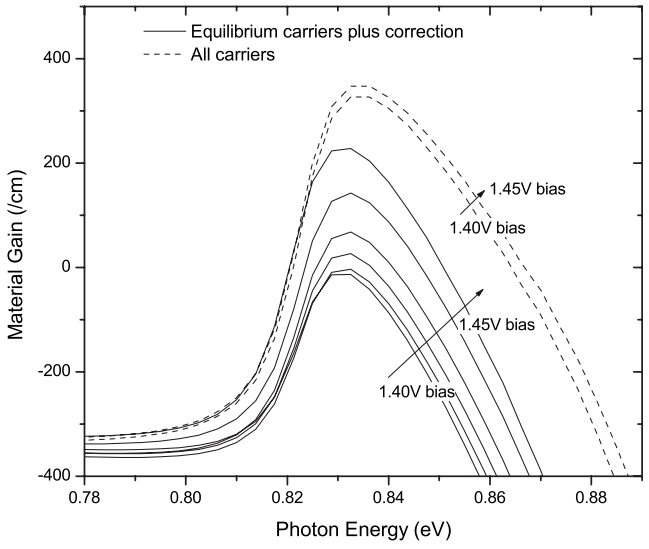

FIG. 3. Gain spectra versus photon energy for a number of applied biases. The solid lines are the gain using the best-fit equilibrium plus the nonequilibrium correction term. Dashed lines are for gain, assuming that the total carrier density in the well is at equilibrium. Capture rate $\gamma=10/\mathrm{ps}$.

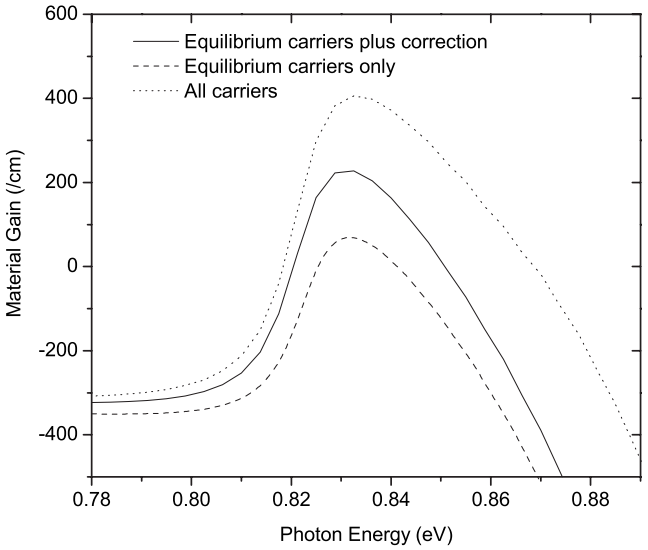

FIG. 4. Gain spectra versus photon energy for a applied bias of 1.45 V. Gain curves are shown for calculations using the best-fit equilibrium plus the nonequilibrium correction term and the best-fit equilibrium only, assuming that the total carrier density in the well is at equilibrium. Capture rate $\gamma=10/\mathrm{ps}$.

whether the best-fit concentration has higher or lower contributions in the lowest lying energy levels. It would also depend on the actual carrier concentrations involved. In all our calculations, total carrier concentrations in the well range from 2.5 to $3.5\times10^{18}/\mathrm{cm}^3$. At this low level, a small change in density can have a significant change on the gain.

To see the effect of the carrier capture term, in Fig. 5, we plot maximum gain versus bias for two capture rates. As expected, the larger the capture rate, the larger the gain because more carriers will scatter into the well. From these results, it is evident that gain is not a linear function of applied bias. After an applied bias of 1.47 V, the maximum gain actually starts to decrease. It is around this bias that the heterostructure potential on the right side of the well is lower

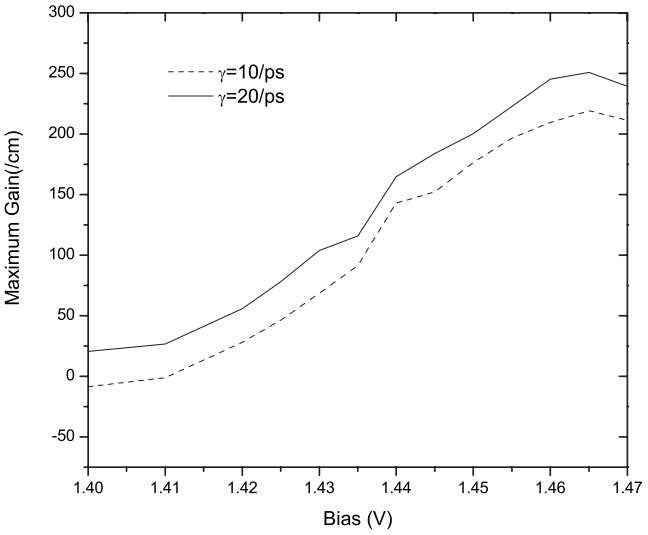

FIG. 5. Maximum gain versus applied bias for two carrier capture rates.

than that on the left side of the well (see Fig. 1). The maximum gain will occur when the left and right potentials are the same. If the left one is lower, carriers will backscatter more, and if the right is lower, there will be more carriers passing over the well. In both cases, there will be less carriers captured by the well.

VII. CONCLUSION

In this paper, we have developed a complete self-consistent laser model based on a combination of Wigner functions for dynamical properties and Green functions for spectral properties. The method was designed this way because Wigner functions are very convenient for the incorporation of boundary conditions, while gain is more conveniently formulated with the Green functions. When one is deciding if this method is appropriate for their simulations, it is neccessary to ask if the additional computational overhead required in this model for the conversion between the Green and Wigner functions is worth it, or would it be quicker to use only Green or Wigner functions exclusively. In the example given, the conversion process is fast because the Wigner functions were calculated in a parabolic model.

We have presented an example where the model has been simplified to providing a nonequilibrium correction term to a standard gain formula. We have shown from this example that we can model both the carrier dynamics and gain. The boundary conditions used in this model were Fermi distribution functions. We could, however, incorporate this into a larger model by using some sort of semiclassical transport model (such as drift diffusion) up to the boundaries of the Wigner functions and then using the semiclassical model's distribution functions as the boundary conditions for the Wigner functions in place of the Fermi distributions used in this work.

Future directions for this method will be to add in phonon and Coulombic interactions in a more detailed way, use a non-Markovian approximation (the easiest approximation would be to use a Markovian approximation for the Wigner functions and a non-Markovian formulation for the Green functions and gain[29]). We could also include the electric field coupling in the Wigner functions and logically use a LK model for the Wigner functions. It would be of interest to apply this model to other types of structures such as quantum dots.

ACKNOWLEDGMENTS

We would like to acknowledge the support from the Natural Science and Engineering Research Council of Canada (NSERC).

[1] M. S. Wartak and P. Weetman, in *Handbook of Semiconductor Nanostructures and Nanodevices*, Nano-Photonics and Optoelectronics Vol. 4, edited by A. A. Balandin and K. L. Wang (American Scientific, Los Angeles, 2006), pp. 409–455.
[2] J. Minch, S. H. Park, T. Keating, and S. L. Chuang, IEEE J. Quantum Electron. **35**, 771 (1999).
[3] R. Nagarajan, M. Ishikawa, T. Fukushima, R. S. Geels, and J. E. Bowers, IEEE J. Quantum Electron. **28**, 1990 (1992).
[4] B. Witzigmann, M. S. Hybertsen, C. L. Reynolds, G. L. Belenky, L. Shterengas, and G. E. Shtengel, IEEE J. Quantum Electron. **39**, 120 (2003).
[5] J. N. Pedersen and A. Wacker, Phys. Rev. B **72**, 195330 (2005).
[6] W. Z. Shangguan, T. C. Au Yeung, Y. B. Yu, and C. H. Kam, Phys. Rev. B **63**, 235323 (2001).
[7] B. A. Biegel and J. D. Plummer, Phys. Rev. B **54**, 8070 (1996).
[8] P. Weetman and M. S. Wartak, J. Comput. Theor. Nanosci. **3**, 463 (2006).
[9] W. R. Frensley, Rev. Mod. Phys. **62**, 745 (1990).
[10] H. Tsuchiya and T. Miyoshi, IEEE J. Quantum Electron. **32**, 865 (1996).
[11] P. Weetman, PhD. Thesis, University of Waterloo, 2002.
[12] W. W. Chow, S. W. Koch, and M. Sargent III, *Semiconductor-Laser Physics* (Springer, Berlin, 1994).
[13] S. L. Chuang, *Physics of Optoelectronic Devices* (Wiley, New York, 1995).
[14] R. Binder and S. W. Koch, Prog. Quantum Electron. **19**, 307 (1995).
[15] J. Hader, J. V. Moloney, and S. W. Koch, IEEE J. Quantum Electron. **35**, 1878 (1999).
[16] P. Weetman and M. S. Wartak, J. Appl. Phys. **93**, 9562 (2003).
[17] G. D. Mahan, *Many-Particle Physics*, 2nd ed. (Plenum, New York, 1990).
[18] A. Wacker, Phys. Rep. **357**, 1 (2002).
[19] H. Tsuchiya and T. Miyoshi, J. Appl. Phys. **83**, 2574 (1998).
[20] R. A. Craig, J. Math. Phys. **9**, 605 (1968).
[21] A. L. Fetter and J. D. Walecka, *Quantum Theory of Many-Particle Systems* (McGraw-Hill, New York, 1971).
[22] P. Weetman and M. S. Wartak (unpublished).
[23] Q. T. Vu, H. Haug, and S. W. Koch, Phys. Rev. B **73**, 205317 (2006).
[24] O. Hess and T. Kuhn, Phys. Rev. A **54**, 3347 (1996).
[25] Weng W. Chow and Stephan W. Koch, IEEE J. Quantum Electron. **41**, 495 (2005).
[26] C. Henry, J. Lightwave Technol. **LT4**, 288 (1986).
[27] B. Tromberg, H. Olesen, and X. Pan, IEEE J. Quantum Electron. **27**, 178 (1991).
[28] M. J. Connelly, IEEE J. Quantum Electron. **37**, 439 (2001).
[29] D. Ahn, IEEE J. Quantum Electron. **32**, 960 (1996).